VIP Chiral Nanomaterials

DOI: 10.1002/anie.201105479

Chiral Nematic Mesoporous Carbon Derived From Nanocrystalline Cellulose**

*Kevin E. Shopsowitz, Wadood Y. Hamad, and Mark J. MacLachlan**

Dedicated to Dr. Richard Berry on the occasion of his 60th birthday

Template synthesis based on the self-assembly of lyotropic liquid crystals offers access to mesoporous solids with high specific surface areas and periodic structures.[1] Incorporating mesopores (i.e., pores ranging from 2 to 50 nm in diameter) into carbonaceous materials may be advantageous for certain applications, including the adsorption of large molecules, electrochemical double-layer capacitors, lithium ion batteries, catalyst supports, and field-effect transistors.[2–6] Ordered mesoporous carbon materials were first synthesized by using ordered mesoporous silica as a hard template.[3a,7] In the hard-templating (also referred to as nanocasting) approach,[8] mesoporous silica is repeatedly infiltrated with a suitable carbon precursor (e.g., sucrose) that is carbonized within the pores of the silica at elevated temperature. After sufficient pore loading and etching of the silica, mesoporous carbon with a structure that is the inverse of the original silica template is obtained. Despite the potential benefits of using mesoporous carbon over traditional activated carbon, the cost of making these materials may be prohibitive. Finding more economical synthetic routes, both in terms of the number of steps involved and precursors used, is important if mesoporous carbon is to be implemented in new technologies.

Direct surfactant-templating approaches (soft templating) have also been developed for the synthesis of mesoporous carbon by condensing polymerizable carbon precursors (e.g., phenolic resins) around block copolymer templates.[9] Soft templating requires fewer synthetic steps than hard templating and offers improved control over the morphology of the mesoporous carbon products. For example, free-standing mesoporous carbon membranes have been synthesized through evaporation-induced self-assembly coupled with soft templating.[10] The specific surface areas of these films, however, are considerably less than those of mesoporous carbons produced by hard templating. The use of both hard- and soft-templating approaches has enabled mesoporous carbon to be synthesized with cubic and hexagonal pore systems that are ultimately derived from the self-assembly of surfactants into ordered mesophases.[11] The synthesis of mesoporous carbon templated by other liquid-crystal phases, for example nematic and chiral nematic phases, has been virtually unexplored. In particular, the incorporation of chiral organization into mesoporous carbon could open the door for applications that involve enantioselective adsorption.

Chiral nematic liquid crystals, which consist of mesogens organized into a long-range helical assembly, exhibit unique properties, such as the selective reflection of circularly polarized light.[12] The incorporation of chiral nematic organization into solid-state materials could give rise to novel properties. Kyotani and co-workers have synthesized graphitic carbon with chiral nematic ordering by first polymerizing polyacetylene within a thermotropic chiral nematic liquid crystal followed by doping with iodine and pyrolysis.[13] It is expected that these materials will display interesting electromagnetic properties.

As the major constituent of plant cell walls, cellulose is the most abundant biological material on the planet. Recently, there has been significant interest in the study of cellulose fibrils with nanometer dimensions that have high surface area and can behave as lyotropic liquid crystals.[14] Stable suspensions of nanocrystalline cellulose (NCC) can be obtained through hydrolysis of bulk cellulosic material with sulfuric acid.[15] In water, suspensions of NCC organize into a chiral nematic phase that can be preserved upon slow evaporation, thereby resulting in chiral nematic films.[16] The unique physical properties and natural abundance of NCC make it attractive as a potential template for porous materials. Although bulk cellulosic materials are commonly used to generate activated carbon, to date there have been no studies on the use of NCC as a template for mesoporous carbon.

Recently, our research group reported that evaporation-induced self-assembly of NCC with different silica precursors can result in composite films with chiral nematic structures, and that the removal of NCC from these films generates chiral nematic mesoporous silica.[17] Herein we report that NCC–silica composite films may also be used to generate mesoporous carbon with a high specific surface area and excellent retention of the chiral nematic organization. This provides the first example of using nanocrystalline cellulose as a template for mesoporous carbon as well as the first demonstration of a mesoporous carbon with chiral nematic ordering. We demonstrate that the use of silica is necessary for both the introduction of mesoporosity and the preservation of the

[*] K. E. Shopsowitz, Prof. Dr. M. J. MacLachlan
Department of Chemistry, University of British Columbia
2036 Main Mall, Vancouver, BC, V6T 1Z1 (Canada)
E-mail: mmaclach@chem.ubc.ca
Dr. W. Y. Hamad
FPInnovations
3800 Wesbrook Mall, Vancouver, BC, V6S 2L9 (Canada)

[**] This work was supported by the Natural Sciences and Engineering Research Council (NSERC) of Canada and FPInnovations. K.E.S. thanks the NSERC for a graduate fellowship.

Supporting information for this article is available on the WWW under http://dx.doi.org/10.1002/anie.201105479.

long-range chiral organization in the carbonized NCC materials. Our approach gives access to high surface area free-standing mesoporous carbon films that are otherwise difficult to obtain, and has the advantage of requiring relatively few synthetic steps (when compared with the usual hard-templating procedure) by utilizing the structural template (NCC) directly as the carbon source.

Our approach is summarized in Figure 1. An aqueous suspension of NCC was mixed with tetramethyl orthosilicate

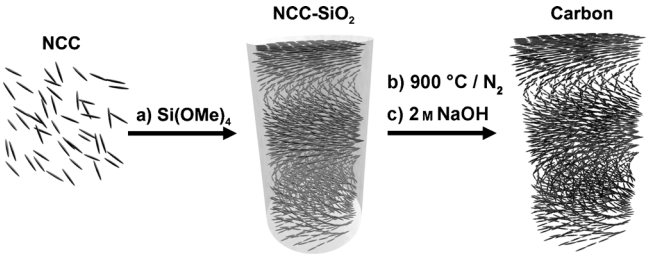

Figure 1. Synthesis of chiral nematic mesoporous carbon. a) NCC prepared by hydrolysis with sulfuric acid is mixed with TMOS and slowly evaporated to form chiral nematic NCC–silica composite films. b) NCC–silica composite films are pyrolyzed in an inert atmosphere at 900 °C to generate carbon–silica composite films. c) Silica is removed from the carbon–silica composite films using 2 M NaOH to generate chiral nematic mesoporous carbon.

(TMOS) and cast into chiral nematic composite films as previously reported (see Figure S1 in the Supporting Information).[17] The NCC–silica composite films were then pyrolyzed under nitrogen at 900 °C to give carbon–silica composite films. The conversion of NCC into carbon proceeded in approximately 30 % yield, as determined by thermogravimetric analysis (TGA; see Figure S2 in the Supporting Information). Some of the carbon–silica composite samples showed iridescence, thus providing evidence for the retention of their chiral nematic organization after carbonization (see Figure S3 in the Supporting Information). In the final step, the silica was dissolved with aqueous NaOH to yield free-standing carbon films with centimeter dimensions and a glossy black appearance (Figure 2 a). After the NaOH treatment, the removal of silica in the samples was confirmed by TGA (performed in air), which typically shows gradual decomposition of the carbon between 500 and 650 °C and a small residual ash of about 3 wt %. Elemental analysis of the materials showed them to generally be around 90 wt % carbon and 1 wt % hydrogen (energy-dispersive X-ray analysis indicates that the remaining 9 wt % consists mostly of oxygen, with trace amounts of sodium and silicon also present). The conversion of NCC into carbon was further studied by powder X-ray diffraction (PXRD) and Raman spectroscopy (see Figure S4 in the Supporting Information). The Raman spectrum shows a broad D band centered at 1320 cm^{-1} that overlaps with a smaller G band at 1595 cm^{-1}, while PXRD shows broad peaks centered at $2\theta \approx 23°$ and 43°. These results are consistent with the conversion of NCC into amorphous carbon.

The porosity of the NCC-derived carbon was analyzed by nitrogen adsorption/desorption and the results are summarized in Table 1. To study the influence of silica on the porosity of the carbon materials, samples were prepared from chiral nematic precursor films with different proportions of NCC and silica. Pyrolysis of NCC films without the addition of any silica precursor (**CMC-1**) resulted in microporous carbon, as shown by a type I adsorption isotherm (Figure 2 b). When the carbon materials were prepared using silica, as shown in Figure 1, the resulting carbon materials displayed isotherms with more type IV character compared to **CMC-1** as well as significant hysteresis, which indicates the introduction of mesoporosity into the samples. A maximum Brunauer–Emmett–Teller (BET) surface area and total pore volume of 1460 $m^2 g^{-1}$ and 1.22 $cm^3 g^{-1}$, respectively, were measured for carbon obtained from a 65 % NCC–silica composite (**CMC-3**, Figure 2 b). Carbon materials prepared from composites with a lower or higher fraction of silica (relative to **CMC-3**) had decreased surface areas and pore volumes (Table 1). It is apparent that a minimal amount of silica is necessary for introducing mesoporosity into the NCC-derived carbon. The decrease in mesoporosity observed at higher silica loadings may be due to thicker silica walls preventing the formation of linkages between the carbon regions during pyrolysis. **CMC-3** shows a type IV isotherm (Figure 2 b) with a peak BJH (Barret–Joyner–Halenda model) pore diameter of 2.9 nm (calculated from the adsorption branch of the

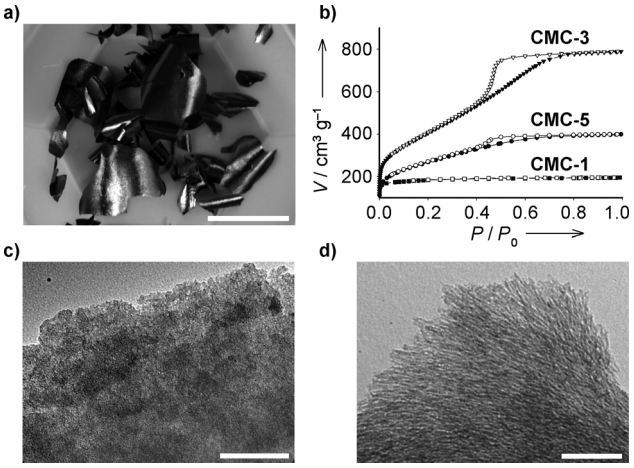

Figure 2. Porosity of different carbon samples. a) Photograph of mesoporous carbon sample **CMC-3** (scale bar = 2 cm). b) N_2 adsorption isotherms of **CMC-1**, **CMC-3**, and **CMC-5**. c) TEM image of **CMC-1** (scale bar = 200 nm). d) TEM image of **CMC-3** (scale bar = 200 nm).

Table 1: Nitrogen adsorption data for different carbon samples prepared from NCC.

Sample	Wt % NCC in composite	BET surface area [$m^2 g^{-1}$]	Micropore area [$m^2 g^{-1}$][a]	Pore volume [$cm^3 g^{-1}$]
CMC-1	100	616	488	0.30
CMC-2	76	578	37	0.38
CMC-3	65	1465	11	1.22
CMC-4	56	1230	128	0.96
CMC-5	43	932	132	0.62

[a] Calculated by *t*-plot analysis of the adsorption branch.

isotherm; see Figure S5 in the Supporting Information). The H2 hysteresis observed for **CMC-3** may indicate some pore blocking and percolation within the mesoporous network. A *t*-plot analysis indicates that **CMC-3** has very little microporosity. Previous reports of mesoporous carbon synthesized by hard templating have shown that microporosity is typically greatest when highly disordered carbon precursors are used (e.g., sucrose).[18] The absence of significant micropores in the carbon walls of **CMC-3** may reflect the highly ordered structure of the individual cellulose nanocrystals prior to carbonization. The microporosity observed for **CMC-1** may result from spaces that form between the individual nanocrystals during carbonization. The mesopores of **CMC-3** were also observed by transmission electron microscopy (TEM, Figure 2d), which shows locally aligned pores, consistent with the local nematic organization expected for a chiral nematic pore structure. The TEM images of **CMC-1**, on the other hand, show much smaller and more disordered pores (Figure 2c).

The long-range chiral nematic structure of **CMC-3** was confirmed by scanning electron microscopy (SEM, Figure 3).

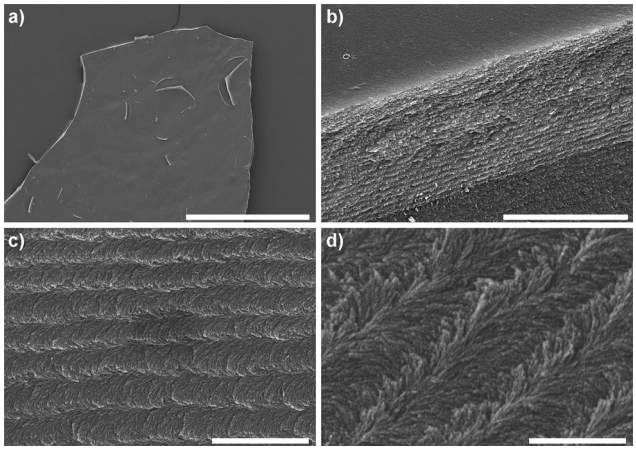

Figure 3. SEM images of **CMC-3**. a) Top view of the film at low magnification (scale bar = 500 μm). b) The side view at the fracture shows a repeating structure perpendicular to the film surface (scale bar = 5 μm). c) Side view of the fracture at higher magnification (scale bar = 2 μm). d) The high-magnification image of the fracture shows a left-handed chiral nematic structure (scale bar = 500 nm).

The chiral nematic ordering of NCC was essentially retained in mesoporous carbon sample **CMC-3** (for an SEM image of a pure NCC film, see Figure S6 in the Supporting Information). The mesoporous carbon films have smooth surfaces with a repeating layered structure perpendicular to the surface. At high magnification we see the rod morphology of NCC retained in the carbon and we observe twisting in a counterclockwise direction, consistent with the left-handed chiral nematic structure of the NCC template (Figure 3d). In contrast, carbon films prepared from chiral nematic NCC films without silica show no retention of chiral nematic ordering (highly disordered layers are seen in some locations, see Figure S7 in the Supporting Information). In addition to introducing mesoporosity into the samples, the silica is also necessary for preserving long-range structural organization in the NCC films during carbonization.

The helical pitch of chiral nematic materials is most often studied by optical techniques, such as polarized optical microscopy and circular dichroism (CD). However, optical studies to probe the chiral nematic structure of **CMC-3** directly could not be carried out because of the intense absorption of light by the carbon films. On the other hand, mesoporous carbon has proven useful as a hard template for metal oxide replica structures as a consequence of the ease with which it can be selectively removed through thermal oxidation.[8] As a proof of concept, we examined whether **CMC-3** could be used to template a chiral nematic silica replica that could be characterized by optical techniques. Silica replication was achieved by using an adapted literature procedure.[19] After multiple loading steps, the carbon–silica films appeared slightly iridescent. The composite films were then pyrolyzed under air to remove the carbon template, thereby yielding small pieces of colorless silica films. Polarized optical microscopy shows that the silica replicas are birefringent, which is indicative of long-range anisotropy (Figure 4a, inset). A strong positive CD signal is observed from the silica replicas with a maximum at 325 nm (Figure 4a), thus demonstrating that they selectively reflect left-

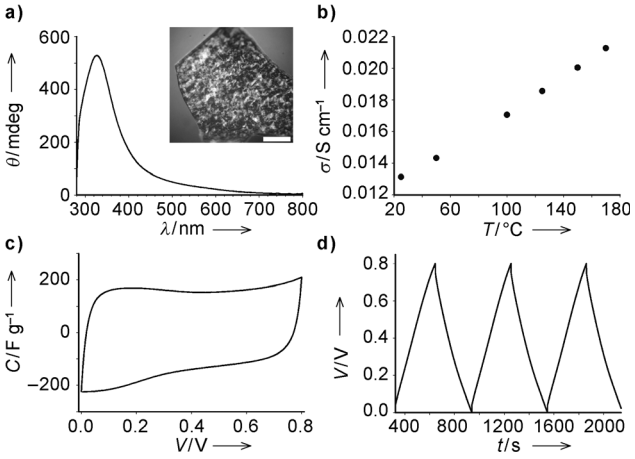

Figure 4. Optical characterization of silica templated by chiral nematic mesoporous carbon **CMC-3** and the capacitor performance of **CMC-3**. a) CD spectrum of silica templated by **CMC-3**. The inset shows a polarized optical microscopy image of the silica viewed under crossed polarizers (scale bar = 200 μm). b) Temperature–conductivity plot of **CMC-3**. c) Cyclic voltammogram of **CMC-3** symmetric capacitor in 1 M H_2SO_4 (scan rate = 2 mV s^{-1}). d) Galvanostatic charge/discharge of **CMC-3** in 1 M H_2SO_4 (current load = 230 mA g^{-1}).

handed circularly polarized light in the UV region. This result gives further confirmation that the left-handed chiral nematic structure of NCC is preserved in the mesoporous carbon and demonstrates that it can be transferred to other materials by hard templating.

An important application for porous carbon materials is in electronic devices. Mesoporous carbon **CMC-3** shows a conductivity of 1.3×10^{-2} S cm^{-1} at 25 °C that increases linearly with increasing temperature over the range 20–

180 °C, which is indicative of semiconducting behavior (Figure 4b). Semiconducting mesoporous carbon has recently been shown to be an effective material for constructing field-effect transistors that could be used in gas-sensor devices.[6] Mesoporous carbons are also promising materials for supercapacitor electrodes. To test the capacitor performance of chiral nematic mesoporous carbon, a symmetrical capacitor was constructed with carbon sample **CMC-3**, using a two-electrode cell with 1 M H_2SO_4 as the electrolyte. The free-standing carbon films were used directly without the addition of any binders. The cyclic voltammogram of **CMC-3** (Figure 4c) shows a rectangular shape with a slight slope, which indicates the occurrence of Faradaic processes (i.e., redox reactions) that likely involve defect functional groups in the material. The galvanostatic charge/discharge profile of **CMC-3** (Figure 4d) shows a symmetrical, triangular shape typical of near-ideal capacitor behavior. The specific capacitance of **CMC-3** calculated from the discharge curve at a current load of 230 $mA\,g^{-1}$ is 170 $F\,g^{-1}$, which is comparable to values reported for hard-templated mesoporous carbons measured under similar conditions.[20] However, **CMC-3** has the advantage that it is more easily synthesized than these materials and is readily obtained as a free-standing film with centimeter dimensions, thereby eliminating the need for a binder.

In summary, we have demonstrated that nanocrystalline cellulose confined within a silica host is an ideal precursor for a new form of mesoporous carbon that has a chiral nematic structure. Upon pyrolysis and etching of the silica, free-standing films of chiral nematic mesoporous carbon are prepared. The chirality of the films was demonstrated by electron microscopy and by using them as a template for chiral nematic silica. As the mesoporous carbon films have a high specific surface area, they are an effective electrode material for supercapacitors. These new carbon films with chiral nematic order may find applications in energy-storage devices, new composite materials, catalyst supports, enantioselective sensors, and adsorption media.

Experimental Section

Preparation of nanocrystalline cellulose (NCC): Fully bleached, commercial kraft softwood pulp was first milled to pass through a 0.5 mm screen in a Wiley mill to ensure uniform particle size and to increase the surface area. The milled pulp was hydrolyzed in sulfuric acid (8.75 mL of a sulfuric acid solution per gram of pulp) at a concentration of 64 wt % and a temperature of 45 °C for 25 min with vigorous stirring. The cellulose suspension was then diluted with cold de-ionized (DI) water (ca. 10 times the volume of the acid solution used) to stop the hydrolysis, and allowed to settle overnight. The clear top layer was decanted and the remaining cloudy layer was centrifuged. The supernatant was decanted and the resulting thick white suspension was washed 3 times with DI water to remove all the soluble cellulose materials. The thick white suspension obtained after the last centrifugation step was placed inside dialysis membrane tubes (12000–14000 molecular weight cut-off) and dialyzed against slow-running DI water for 1–4 days. The membrane tubes containing the extracted cellulose materials were placed periodically in DI H_2O, and the procedure was continued until the pH of the water became constant over a period of one hour. The suspension from the membrane tubes was dispersed by ultrasound treatment in a Fisher Sonic Dismembrator (Fisher Scientific) for 10 min at 60 % power and then diluted to the desired concentration.

Preparation of nanocrystalline cellulose–silica composite films: A 3.5 wt % aqueous NCC suspension (30 mL, pH 2.4) was sonicated for 10 min using an Aquasonic 50T sonic cleaner. Tetramethoxysilane (1.40 mL, 9.5 mmol) was added to the NCC suspension and the mixture was stirred at room temperature for 1 h to allow the formation of a homogeneous mixture. Portions (5 mL) were then transferred to small (60 mm) polystyrene Petri dishes and allowed to evaporate under ambient conditions until solid films had formed (typically ca. 24 h) to give NCC–silica composites with chiral nematic organization. This procedure gave films with 65 wt % NCC (**CMC-3**). Additional samples were prepared by using an identical procedure except for varying the amount of TMOS used to obtain films with different relative amounts of NCC and silica.

For pyrolysis of the cellulose, the composite films (1.0 g) were heated at a rate of 2 °C min^{-1} to 100 °C under flowing nitrogen, held at 100 °C for 2 h, then heated to 900 °C at 2 °C min^{-1} and held at 900 °C for 6 h. After slowly cooling the sample to room temperature, 505 mg of free-standing carbon–silica composite films were recovered. Control sample **CMC-1** was prepared by pyrolyzing a pure NCC film under these conditions. To remove the silica, the carbon–silica composite films (500 mg) were placed in a beaker containing 2 M sodium hydroxide (aqueous, 200 mL) and heated to 90 °C for 4 h. The films were then recovered by filtration and rinsed with copious amounts of water. After drying the sample in air, 175 mg of free-standing mesoporous carbon films were recovered.

The electrical conductivity of the mesoporous films was measured by using the standard four-probe method. Hewlett–Packard model 34401A and 3478A multimeters were used to measure the voltage and current, respectively. The temperature-dependence of the electrical conductivity was measured by varying the temperature of the film placed on a surface equipped with a temperature-controlled heater over a range of 20 to 180 °C.

Electrochemical measurements were carried out on a Brinkmann PGSTAT12 Autolab potentiostat. Dry mesoporous carbon films were weighed and then placed in a 1 M aqueous sulfuric acid solution and allowed to soak for at least 18 h. Two films were then sandwiched in a Swagelok two-electrode cell with a nafion membrane separator and stainless-steel collectors.

Received: August 3, 2011
Published online: September 23, 2011

Keywords: carbon · cellulose · liquid crystals · mesoporous materials · self-assembly

[1] a) C. T. Kresge, M. E. Leonowicz, W. J. Roth, J. C. Vartuli, J. S. Beck, *Nature* **1992**, *359*, 710–712; b) P. Yang, D. Zhao, D. I. Margolese, B. F. Chmelka, G. D. Stucky, *Nature* **1998**, *396*, 152–155.
[2] S. Han, K. Sohn, T. Hyeon, *Chem. Mater.* **2000**, *12*, 3337–3341.
[3] a) J. Lee, S. Yoon, T. Hyeon, S. M. Oh, K. B. Kim, *Chem. Commun.* **1999**, 2177–2178; b) P. Simon, Y. Gogotsi, *Nat. Mater.* **2008**, *7*, 845–854.
[4] a) Y.-S. Hu, P. Adelhelm, B. M. Smarsly, S. Hore, M. Antonietti, J. Maier, *Adv. Funct. Mater.* **2007**, *17*, 1873–1878; b) X. Ji, K. T. Lee, L. F. Nazar, *Nat. Mater.* **2009**, *8*, 500–506.
[5] S. H. Joo, S. J. Choi, I. Oh, J. Kwak, Z. Liu, O. Terasaki, R. Ryoo, *Nature* **2001**, *412*, 169–172.
[6] L. Liao, M. Zheng, Z. Zhang, B. Yan, X. Chang, G. Ji, Z. Shen, T. Wu, J. Cao, J. Zhang, H. Gong, J. Cao, T. Yu, *Carbon* **2009**, *47*, 1841–1845.
[7] R. Ryoo, S. H. Joo, S. Jun, *J. Phys. Chem. B* **1999**, *103*, 7743–7746.

[8] a) M. Tiemann, *Chem. Mater.* **2008**, *20*, 961 – 971; b) A. H. Lu, F. Schüth, *Adv. Mater.* **2006**, *18*, 1793 – 1805.
[9] C. D. Liang, K. Hong, G. A. Guiochon, J. W. Mays, S. Dai, *Angew. Chem.* **2004**, *116*, 5909 – 5913; *Angew. Chem. Int. Ed.* **2004**, *43*, 5785 – 5789.
[10] a) K. Kimijima, A. Hayashi, I. Yagi, *Chem. Commun.* **2008**, 5809 – 5811; b) X. Wang, Q. Zhu, S. M. Mahurin, C. D. Liang, S. Dai, *Carbon* **2010**, *48*, 557 – 570.
[11] a) Y. Meng, D. Gu, F. Zhang, Y. Shi, L. Cheng, D. Feng, Z. Wu, Z. Chen, Y. Wan, A. Stein, D. Zhao, *Chem. Mater.* **2006**, *18*, 4447 – 4464; b) S. Jun, S. H. Joo, R. Ryoo, M. Kruk, M. Jaroniec, Z. Liu, T. Ohsuna, O. Terasaki, *J. Am. Chem. Soc.* **2000**, *122*, 10712 – 10713; c) C. D. Liang, Z. Li, S. Dai, *Angew. Chem.* **2008**, *120*, 3754 – 3776; *Angew. Chem. Int. Ed.* **2008**, *47*, 3696 – 3717.
[12] H. L. de Vries, *Acta Crystallogr.* **1951**, *4*, 219 – 226.
[13] a) K. Akagi, G. Piao, S. Kaneko, K. Sakamaki, H. Shirakawa, M. Kyotani, *Science* **1998**, *282*, 1683 – 1686; b) M. Kyotani, S. Matsushita, T. Nagai, Y. Matsui, M. Shimomura, A. Kaito, K. Akagi, *J. Am. Chem. Soc.* **2008**, *130*, 10880 – 10881.
[14] For a recent review, see D. Klemm, F. Kramer, S. Moritz, T. Lindstrom, M. Ankerförs, D. Gray, A. Doris, *Angew. Chem.* **2011**, *123*, 5550 – 5580; *Angew. Chem. Int. Ed.* **2011**, *50*, 5438 – 5466.
[15] W. Y. Hamad, T. Q. Hu, *Can. J. Chem. Eng.* **2010**, *88*, 392 – 402.
[16] a) J. F. Revol, H. Bradford, J. Giasson, R. H. Marchessault, D. G. Gray, *Int. J. Biol. Macromol.* **1992**, *14*, 170 – 172; b) J. F. Revol, L. Godbout, D. G. Gray, *J. Pulp Pap. Sci.* **1998**, *24*, 146 – 149; c) J. Pan, W. Y. Hamad, S. K. Strauss, *Macromolecules* **2010**, *43*, 3851 – 3858.
[17] K. E. Shopsowitz, H. Qi, W. Y. Hamad, M. J. MacLachlan, *Nature* **2010**, *468*, 422 – 425.
[18] R. Ryoo, S. H. Joo, M. Kruk, M. Jaroniec, *Adv. Mater.* **2001**, *13*, 677 – 681.
[19] A.-H. Lu, W. Schmidt, A. Taguchi, B. Spliethoff, B. Tesche, F. Schüth, *Angew. Chem.* **2002**, *114*, 3639 – 3642; *Angew. Chem. Int. Ed.* **2002**, *41*, 3489 – 3492.
[20] a) A. B. Fuertes, F. Pico, J. M. Rojo, *J. Power Sources* **2004**, *133*, 329 – 336; b) A. B. Fuertes, G. Lota, T. A. Centeno, E. Frackowiak, *Electrochim. Acta* **2005**, *50*, 2799 – 2805.

